Incorporation of histone deacetylase inhibition into the structure of a nuclear receptor agonist

Luz E. Tavera-Mendoza*, Tan D. Quach†, Basel Dabbas‡, Jonathan Hudon†, Xiaohong Liao†, Ana Palijan‡, James L. Gleason†§, and John H. White*‡§

Departments of *Medicine and ‡Physiology, McIntyre Building, McGill University, 3655 Drummond Street, Montreal, QC, Canada H3G 1Y6; and †Department of Chemistry, Otto Maass Building, McGill University, 801 Sherbrooke Street West, Montreal, QC, Canada H3A 2K6

Edited by Pierre Chambon, Institut de Génétique et de Biologie Moléculaire et Cellulaire, Strasbourg, France, and approved April 1, 2008 (received for review September 29, 2007)

1,25-dihydroxyvitamin D_3 (1,25D) regulates gene expression by signaling through the nuclear vitamin D receptor (VDR) transcription factor and exhibits calcium homeostatic, anticancer, and immunomodulatory properties. Histone deacetylase inhibitors (HDACis) alter nuclear and cytoplasmic protein acetylation, modify gene expression, and have potential for treatment of cancer and other indications. The function of nuclear receptor ligands, including 1,25D, can be enhanced in combination with HDACi. We designed triciferol, a hybrid molecule in which the 1,25D side chain was replaced with the dienyl hydroxamic acid of HDACi trichostatin A. Triciferol binds directly to the VDR, and functions as an agonist with 1,25D-like potency on several 1,25D target genes. Moreover, unlike 1,25D, triciferol induces marked tubulin hyperacetylation, and augments histone acetylation at concentrations that largely overlap those where VDR agonism is observed. Triciferol also exhibits more efficacious antiproliferative and cytotoxic activities than 1,25D in four cancer cell models *in vitro*. The bifunctionality of triciferol is notable because (*i*) the HDACi activity is generated by modifying the 1,25D side chain without resorting to linker technology and (*ii*) 1,25D and HDACi have sympathetic, but very distinct biochemical targets; the hydrophobic VDR ligand binding domain and the active sites of HDACs, which are zinc metalloenzymes. These studies demonstrate the feasibility of combining HDAC inhibition with nuclear receptor agonism to enhance their therapeutic potential.

HDAC inhibitors | multiple ligands | vitamin D

The biologically active metabolite of vitamin D_3, 1α,25-dihydroxyvitamin D_3 (1,25D, **1**) (Fig. 1), is best known as a primary regulator of calcium homeostasis (1, 2). However, 1,25D also controls cell differentiation and proliferation through binding to the nuclear vitamin D receptor (VDR) (NR1I1), which regulates histone acetylation, chromatin remodelling and recruitment of RNA polymerase II and ancillary factors required for target gene transcription (2). In addition to their calcium homeostatic properties, 1,25D analogs have therapeutic potential in treatment of hyperproliferative disorders, such as cancer and psoriasis (2, 3). 1,25D analogs may also be effective in treatment of a range of disorders with autoimmune components such as multiple sclerosis, type 1 diabetes and Crohn's disease, an inflammatory bowel disorder (2, 4). Moreover, 1,25D is also a direct inducer of antimicrobial innate immunity (5–7), a finding that has provided a molecular genetic basis for its activity against *Mycobacterium tuberculosis* infections (8).

Recent studies demonstrated combinatorial effects of trichostatin A (TSA, **2**; Fig. 1), a histone deacetylase inhibitor (HDACi), and 1,25D on the proliferation of 1,25D-resistant cancer cells (ref. 9 and L.E.T.-M., B.D., and J.H.W. unpublished results). HDACis, including TSA and suberoylanilide hydroxamic acid (SAHA, **5**) (Fig. 1), regulate the acetylation state of histones and other nuclear and nonnuclear proteins. Like VDR agonists, HDACis modulate gene expression and induce cell cycle arrest, cellular differentiation, and/or apoptosis (10–12), and so they have been investigated as treatments for cancer. The potential of HDACis as therapeutics is underscored by the recent approval of SAHA, under the trade name Zolinza, for treatment of cutaneous T cell lymphoma (13).

In developing therapies against human disease, it is often advantageous to target two or more sympathetic biological targets. The potential advantages of this approach include targeting sympathetic biochemical pathways involved in a disease, limiting the development of resistance and reducing dosages of more toxic drugs. Classical examples include combining reverse transcriptase inhibitors with protease inhibitors in the treatment of AIDS (14) or coadministration of niacin with a statin in the treatment of hypercholesterolemia (15). Although many examples exist where combination therapy involves administration of multiple drugs, there is growing interest in developing "multiple ligands," single chemical entities that interact with multiple biological targets (16). Although achieving appropriate dosing against individual targets is more readily achieved with separate chemical agents, a multiple ligand may have significant advantages. Development of a multiple ligand simplifies analysis of dose/toxicity relationships and pharmacokinetic profiles, holds the potential to localize activity against one target based on affinity for a second target (17), and can improve adherence to a treatment regimen.

Based on the observed synergy between 1,25D and TSA, we sought to combine VDR agonist activity and HDAC inhibition within a single molecule. This presented a significant design challenge. Although many multiple ligands have been designed to interact with two related biological targets [e.g., vasopeptidase inhibitors, which are dual inhibitors of zinc metallopeptidases neprilysin and angiotensin converting enzyme (18)], few have been rationally designed to interact with two markedly different biological targets. In the case of targeting of both the VDR and HDACs, metalloenzyme inhibition would need to be incorporated into the structure of a lipophilic nuclear receptor agonist (19). Further increasing the challenge, 1,25D is fully enclosed within the VDR binding pocket and thus a fully merged structure with overlapping pharmacophores would be necessary. In this article, we describe the design, synthesis, and biochemical characterization of triciferol, a multiple ligand agent that combines VDR agonism and HDAC inhibition to enhance the cytostatic and cytotoxic activities of 1,25D.

Author contributions: L.E.T.-M., T.D.Q., B.D., J.H., X.L., and A.P. performed research; J.L.G. and J.H.W. designed research; J.L.G. and J.H.W. analyzed data; and J.L.G. and J.H.W. wrote the paper.

The authors declare no conflict of interest.

This article is a PNAS Direct Submission.

Freely available online through the PNAS open access option.

§To whom correspondence may be addressed. E-mail: jim.gleason@mcgill.ca or john.white@mcgill.ca.

This article contains supporting information online at www.pnas.org/cgi/content/full/0709279105/DCSupplemental.

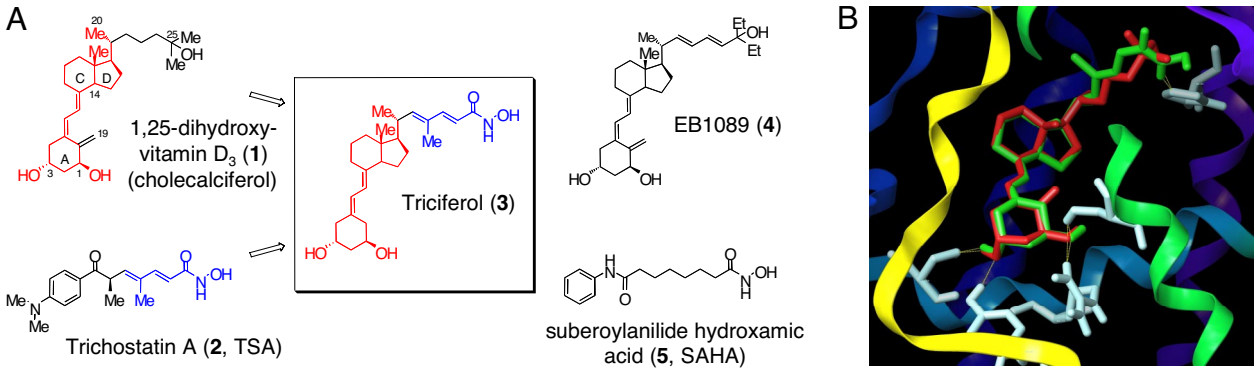

Fig. 1. Design of triciferol. (*A*) Structures of 1,25D (**1**) and TSA (**2**), which are merged into triciferol (**3**). 1,25D analog EB1089 (**4**), HDACi SAHA (**5**) are also shown. (*B*) Triciferol is fully enclosed within the VDR ligand binding domain pocket. Ribbon diagram of the VDR backbone with overlays of docking of 1,25D (red) and triciferol (green). Note that a portion of helix 3 (in green) has been removed for clarity. Key hydrogen bonding amino acids are shown in white. Hydrogen bonds are indicated by fine lines.

Results

Design of Triciferol. Triciferol (**3**) (Fig. 1) was designed with the aid of structure/activity data for both 1,25D and its analogs, and HDACis TSA and SAHA. Numerous 1,25D analogs, including seocalcitol (EB1089, **4**) (Fig. 1), have revealed that the VDR can accommodate structures with alterations in side chain substitution and length (19–21), as long as critical hydrogen bonds are maintained at all three hydroxyl groups. HDACis, such as TSA and SAHA, are composed of highly variable "cap" structures that bind at the surfaces of HDACs, coupled via a linking chain to hydroxamic acids (22, 23) or other groups (24) that chelate active site zinc ions. Triciferol combines the secosteroidal backbone of 1,25D with the dienyl hydroxamic acid of TSA. It was expected that the hydroxamic acid would act as a surrogate for the 25OH group and establish hydrogen bonds to His-305 and/or His-397 in the VDR ligand binding pocket, an essential element of 1,25D binding to the receptor (19). Indeed, optimal docking solutions (AutoDock 3.0, FITTED 2.0) indicated that triciferol should bind to the VDR in an orientation roughly similar to 1,25D (25, 26), with the side chain hydroxamic acid rotated relative to the 25-hydroxyl of 1,25D, but still forming a strong hydrogen bond between the hydroxamate OH and His-397 (Fig. 1*B*). The secosteroidal core overlays almost exactly that of VDR-bound 1,25D, maintaining hydrogen bonds to the 1- and 3-OH groups (27). The computational models predicted that the affinity of triciferol for VDR should be similar to that of 1,25D and EB1089. No preliminary modeling was conducted on the HDAC binding site because of poor handling of zinc-hydroxamic acid interactions in all modeling methods. However, given the breadth of HDACi cap group structures reported (22–24), it was reasonable to expect that the secosteroidal core of triciferol could serve effectively in this capacity when combined with the known affinity of the dienyl hydroxamic acid for HDACs.

Synthesis and Bifunctional Activity of Triciferol. Triciferol was synthesized in 10 steps (Fig. 2) from vitamin D_2 (**6**) and A-ring phosphine oxide **8** (28), after a general sequence of ozonolytic degradation of vitamin D_2, installation of the A-ring via Horner coupling, extension of the side chain by sequential Wittig olefination and hydroxamic acid formation via the acid chloride

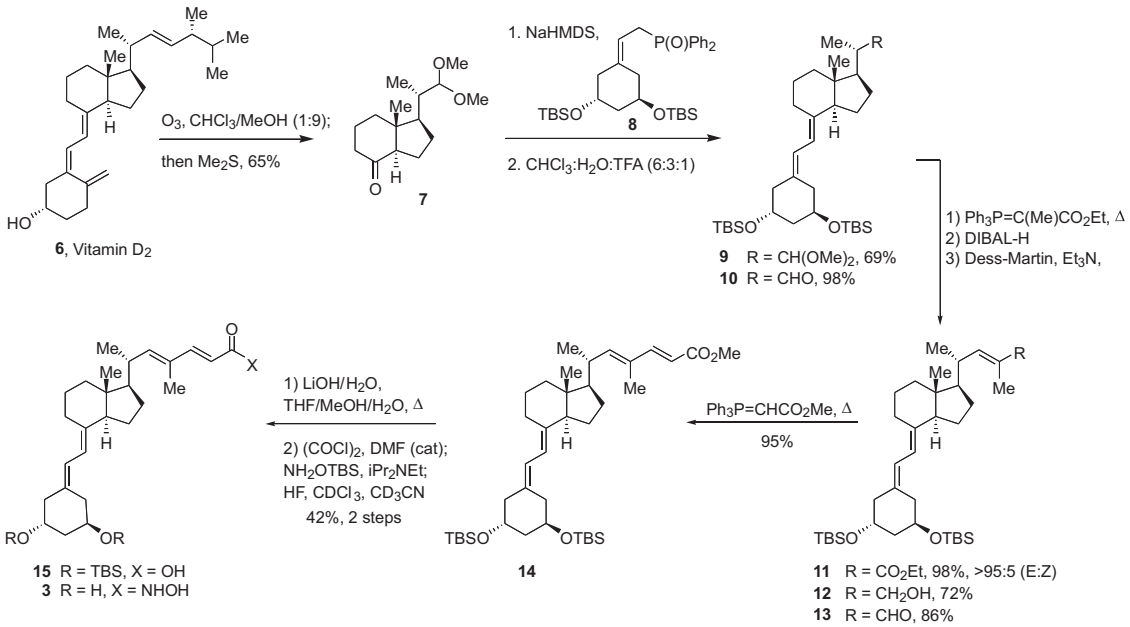

Fig. 2. Schematic representation of key elements of the synthesis of triciferol (see *SI Materials and Methods* and Scheme S1 for details of synthesis).

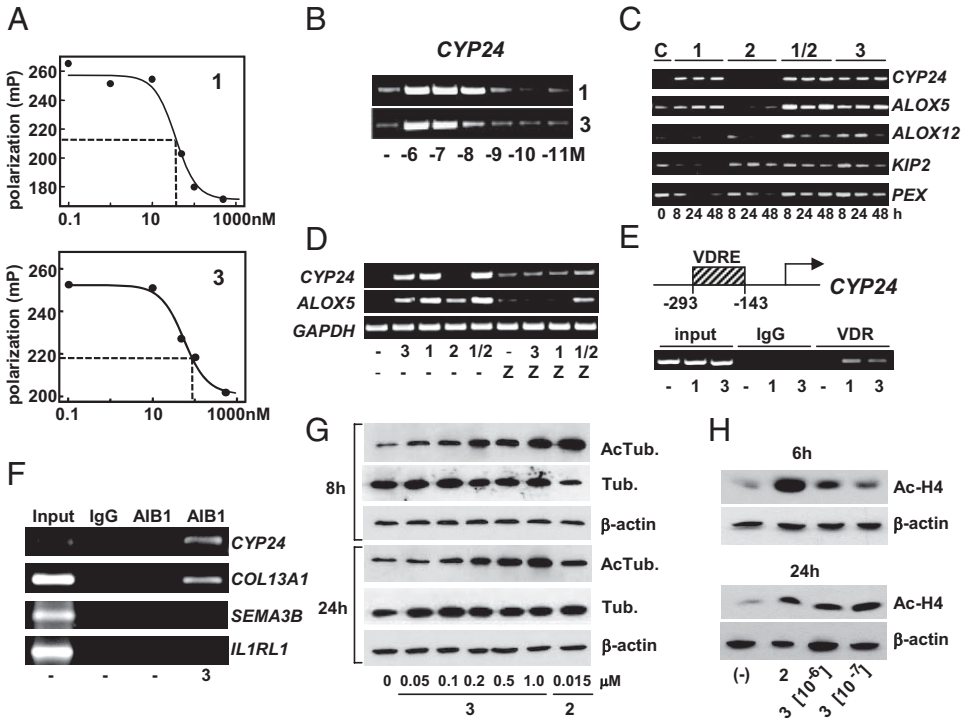

Fig. 3. VDR agonist and HDACi activities of triciferol. (*A*) Triciferol binds directly to the VDR ligand binding domain. Fluorescence polarization competition assays comparing displacement of a fluorescent tracer from the VDR ligand binding domain are shown. (mP, milli-polarization units; see *SI Materials and Methods* for assay details). Estimated IC50s for 1,25D and triciferol in the assay were 32 and 87 nM, respectively. (*B*) Dose-response analysis of induction of *cyp24* expression by 1,25D (**1**) and triciferol (**3**). (*C*) Comparison of the regulation of 1,25D target genes by 100 nM 1,25D (**1**), 15 nM TSA (**2**), 1,25D and TSA together (**1**+**2**), and 100 nM triciferol (**3**). (*D*) VDR antagonist ZK159222 blocks triciferol-induced expression of 1,25D target genes *cyp24* and *alox5*. Cells were treated with vehicle (−), 1,25D (**1**), TSA (**2**), triciferol (**3**), and/or ZK159222 (Z), as indicated. (*E*) (*Upper*) Schematic representation of the proximal human *cyp24* promoter. (*Lower*) Analysis of induction by 100 nM 1,25D (**1**) or triciferol (**3**) of VDR binding to the 1,25D-responsive region of the human *cyp24* promoter by ChIP assay. (*F*) Re-ChIP analysis of recruitment induced by triciferol of the coactivator AIB1 to 1,25D target genes in MCF-7 cells, which overexpress AIB1 (36). The VDR was immunoprecipitated from extracts prepared for ChIP assays and reimmunoprecipitated with an antibody directed against AIB1. (*G*) Western blot analysis of dose-dependent induction of tubulin acetylation in SCC4 cells by triciferol (**3**) in SCC4 cells. Blots were probed for both total tubulin and actin as controls. (*H*) Western analysis of induction of histone H4 acetylation after 8 or 24 h of treatment with TSA (**2**) or triciferol (**3**), as indicated. See *SI Materials and Methods* for details.

[Fig. 2; see supporting information (SI) *Materials and Methods* for complete details]. Direct binding of triciferol to the VDR was assessed by using a fluorescence polarization competition (FPC) assay, which revealed that triciferol competed for tracer binding with an apparent IC50 of 87 nM or ≈3-fold higher than that of 1,25D (32 nM) (Fig. 3*A*). VDR agonism of triciferol was tested initially by using a 1,25D-sensitive reporter gene assay, which revealed agonist activity comparable to that of 1,25D at 100 nM (Fig. S1). VDR agonism was also assessed in human squamous carcinoma SCC4 cells (29, 30) by analyzing induction of the gene encoding CYP24 (Fig. 3*B*), the enzyme that initiates 1,25D catabolism (1, 2). Triciferol induced strong *cyp24* expression and was within a factor of ≈10 as potent as 1,25D, in good agreement with the results of the FPC assay.

We compared further the capacity of triciferol and a combination of 1,25D and TSA to regulate the expression of a series of $1,25D_3$ target genes (31, 32) in SCC4 cells over 48 h. This revealed profiles of gene regulation by triciferol that are more similar to those of 1,25D and TSA in combination than 1,25D alone (Fig. 3*C*). *Cyp24* was completely unresponsive to TSA, and its induction by 1,25D, 1,25D and TSA or triciferol did not differ substantially. However, in many cases, the magnitude of gene expression observed in the presence of triciferol differed markedly from that of 1,25D under conditions where TSA was active on its own or where it substantially enhanced $1,25D_3$-dependent gene regulation (*cdkn1c*/*kip2*, *alox12*, and *pex*). Notably, unlike 1,25D, triciferol induced a marked up-regulation of the gene encoding cyclin-dependent kinase inhibitor $p57^{KIP2}$ (*cdkn1c*/*kip2*), whose expression is lost during oral SCC progression (33). Induction of *cyp24* and *alox5* by triciferol was markedly inhibited by the VDR antagonist ZK159222 (Fig. 3*D*), consistent with a VDR-driven mechanism of gene regulation. Furthermore, treatment with either 1,25D or triciferol markedly enhanced VDR binding to the promoter-proximal VDRE region (34) of the *cyp24* promoter, as assessed by chromatin immunoprecipitation (ChIP) assay (Fig. 3*E*), consistent with their similar effects on *cyp24* induction. In other ChIP assays, triciferol also induced VDR binding to the VDRE (32) in the *col13a1* gene (data not shown). Moreover, re-ChIP experiments revealed that triciferol induced recruitment of the p160 coactivator AIB1 (35) to VDR-bound target genes (Fig. 3*F*). Taken together, the results above show that triciferol is a VDR agonist with a gene regulatory profile that is distinct from that of 1,25D.

In preliminary assays with an acetylated colorimetric substrate (36), triciferol showed clear inhibitory activity (Fig. S2). In control experiments in SCC4 squamous carcinoma cells, 1,25D alone at concentrations as high as 1 μM did not alter tubulin or histone acetylation and had no substantial effect on hyperacetylation induced by TSA (Fig. S3). In contrast, treatment of SCC4 cells with triciferol induced a marked dose-dependent increase in levels of acetylated α-tubulin (Fig. 3*G*) and enhanced acetylation of histone H4 (Fig. 3*H*). Tubulin hyperacetylation (Fig. 3*G*) was visible after 8 h of incubation with triciferol concentrations as low as 50 nM, and plateaued at a concentration of

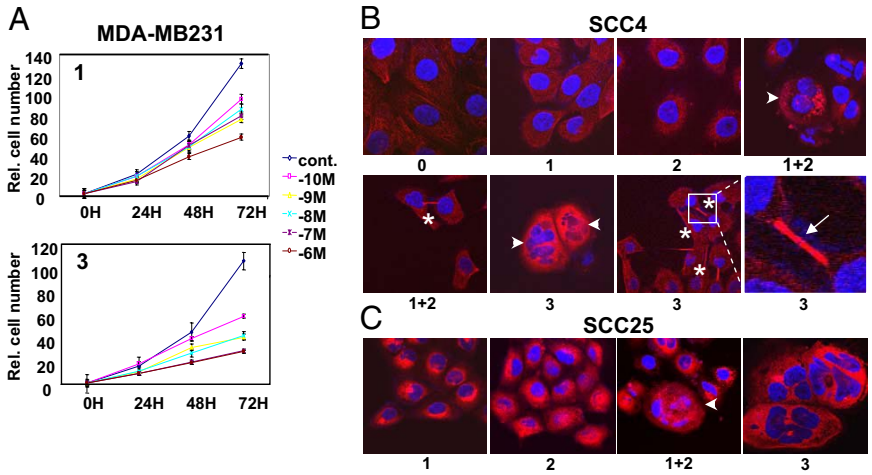

Fig. 4. Analysis of the antiproliferative and cytotoxic activities of triciferol. (*A*) Comparison of the dose-dependent effects of 1,25D (**1**) and triciferol (**3**) on proliferation of human MDA-MB231 breast cancer cells. Growth inhibition by triciferol was statistically significantly different from that of 1,25D at concentrations of 1 nM or above. (*B*) 1,25D (**1**) and TSA (**2**) in combination or triciferol (**3**) alone induces morphological changes in human SCC4 cells associated with mitotic catastrophe. Multinucleated cells are indicated by arrowheads. Cells joined by tubulin ''bridges'' are indicated by asterisks. (*Lower Right*) Higher magnification image of the adjacent panel of a tubulin bridge (arrow) joining two cells. (*C*) Experiments similar to those in B showing multinucleation (arrowheads) in human SCC25 cells treated with 1,25D (**1**) and TSA (**2**) in combination or triciferol (**3**). Immunocytochemistry on SCC4 and SCC25 cells was performed by using rabbit anti-human α/β tubulin. All samples were counterstained with Hoechst dye. See *SI Materials and Methods* for details.

≈200 nM, concentrations that largely overlap those where VDR agonism is observed (Fig. 3*B*).

Triciferol Exhibits Enhanced Cytostatic and Cytotoxic Activities. We compared further the capacity of triciferol and 1,25D to control proliferation and viability of cancer cell lines. Triciferol was significantly more efficacious in suppressing the proliferation of estrogen receptor-negative human MDA-MB231 breast cancer cells (Fig. 4*A*). Similar results were obtained in human SCC4 cells (data not shown). 1,25D treatment decreased the numbers of SCC4 cells in S phase of the cell cycle, and induced a partial accumulation in G_0/G_1. In contrast, triciferol reduced the number of cells in S, but induced an accumulation in G_2/M, effects that were similar to those induced by 1,25D and TSA together (Fig. S4).

Given the marked effect of triciferol on tubulin acetylation and the association of tubulin acetylation with microtubule stabilization, we analyzed the effects of various treatments on tubulin morphology in SCC4 cells to determine whether treatment with triciferol disrupted microtubule dynamics. Treatment with 1,25D or TSA alone did not induce distinct morphological changes (Fig. 4*B*), whereas treatment with 1,25D and TSA together produced a range of effects, including large variations in cell size and shape, asymmetric cell divisions and occasional multinucleated cells (Fig. 4*B*, arrowheads, and data not shown). Unlike 1,25D, triciferol also induced the formation of multinucleated cells (Fig. 4*B*, arrowheads). Moreover, 1,25D and TSA in combination or triciferol alone induced formation of numerous intercellular tubulin "bridges" (Fig. 4*B*, asterisks), reminiscent of collapsed telophase mitotic spindles (Fig. 4*B*, arrow). In contrast, although triciferol or 1,25D and TSA in combination induced frequent multinucleation in well differentiated SCC25 head and neck squamous carcinoma cells (Fig. 4*C*), we found no evidence for formation of intercellular tubulin bridges. The observations of partial G_2/M arrest, formation of multinucleated cells, and collapsed mitotic spindles in the presence of triciferol are consistent with death by mitotic failure in SCC4 cells. Note that none of the treatments markedly induced the expression of markers of apoptosis, such as annexin V, although triciferol markedly enhanced the capacity of UV light, which induces apoptosis in SCC4 cells, to induce annexin V expression (Fig. S5).

The cytotoxic properties of triciferol were further analyzed in the human MCF-7 breast cancer cell model. MCF-7 cells are estrogen receptor α-positive and are sensitive to autophagic cell death induced by a number of agents including antiestrogens and EB1089 (37, 38). Treatment of MCF-7 cells with triciferol induced ≈2.5-fold higher rates of cell death than equimolar amounts of 1,25D (Fig. 5*A*). Staining for annexin V indicated that the elevated cell death was not due to apoptosis (Fig. S6). Rather, 1,25D and TSA combined, or triciferol induced markedly enhanced formation of autophagosomes in MCF-7 cells, as judged by lysotracker red staining (Fig. 5*B*), consistent with autophagy.

Discussion

Nuclear receptor ligands, such as 1,25D, have attracted intensive interest in the pharmaceutical industry because of their diverse physiological functions, clinical relevance, and synthetic accessibility. HDACis have therapeutic potential on their own and enhance the function of other therapeutics, including nuclear receptor ligands, in both experimental cancer models and in the clinic (39, 40). For example, HDACis augment the therapeutic effects of retinoids in retinoid-resistant promyelocytic leukemia (39) and have been shown to enhance the sensitivity of breast cancers cells to antiestrogens (41, 42). Our results demonstrate that triciferol functions as a multiple ligand with combined VDR agonist and HDAC antagonist activities. As a VDR agonist, it acts on several target genes with a potency within an order of magnitude of that of 1,25D, but with a gene regulatory profile closer to that of 1,25D and TSA in combination than to 1,25D alone. These studies also underline the flexibility in design of potential HDACi, because the secosteroidal backbone of triciferol is capable of playing the role of the HDACi "cap" structure. Intriguingly, fusion of the dienyl hydroxamic acid of TSA to the secosteroidal backbone of vitamin D alters HDACi specificity as triciferol appears to be more selective for inducing tubulin hyperacetylation than TSA, and future experiments will be needed to establish activity of triciferol against specific HDAC isozymes.

A significant concern when designing multiple ligands is the difficulty in matching potency for individual targets. Importantly, we found that triciferol induces protein hyperacetylation

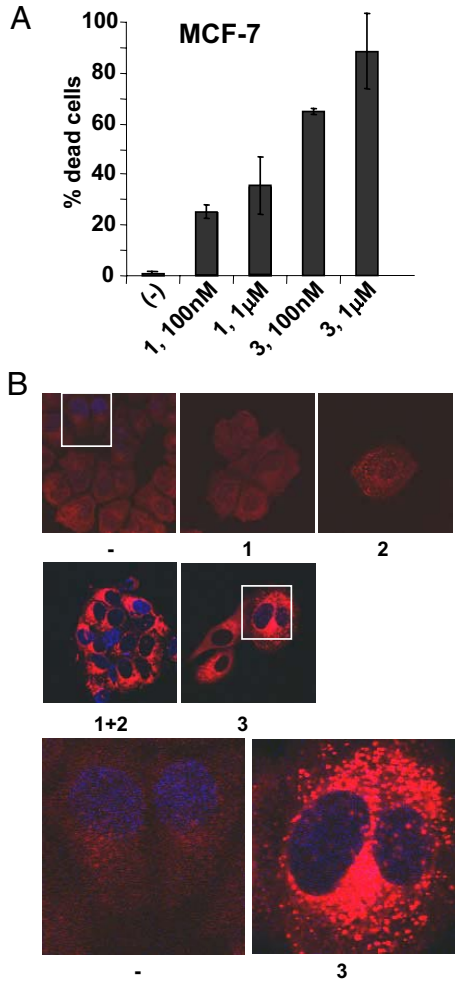

Fig. 5. Comparison of autophagic cell death induced by 1,25D and triciferol in human MCF-7 breast cancer cells. (*A*) MCF-7 cell death induced by 1,25D (**1**) or triciferol (**3**) as measured by trypan blue exclusion assay. (*B*) Analysis of formation of autophagosomes in MCF-7 cells treated with vehicle (−), 1,25D (**1**), TSA (**2**), 1,25D and TSA together (**1**+**2**), or triciferol (**3**). (*Lower*) Magnifications of the boxed regions of control or triciferol-treated cells. See *SI Materials and Methods* for details.

in a concentration range largely overlapping that where VDR agonism is observed, and that this hyperacetylation is sustained over at least 24 h. Thus, it might be expected that it would function as an effective multiple ligand *in vivo*. Indeed, triciferol exhibited enhanced cytostatic properties relative to 1,25D in poorly differentiated breast and squamous carcinoma lines and displayed enhanced cytotoxic properties in the MCF-7 breast cancer line. Moreover, although treatment with 1,25D or TSA alone did not have marked effects on SCC4 cell morphology, triciferol induced morphological changes that were very similar to those seen with combined treatment with 1,25D and TSA. Taken together, these data show that triciferol acts as a multiple ligand with significantly enhanced properties relative to either 1,25D or TSA alone in the models tested. The data also suggest that triciferol may exhibit enhanced therapeutic potential relative to 1,25D or other analogues.

Although we have focused here on cancer models, compounds like triciferol may have enhanced activities against other indications targeted by 1,25D or its analogs, such as psoriasis (2), microbial infections (5–8), or autoimmune conditions, such as inflammatory bowel diseases (4). An important next step is to compare the therapeutic index of triciferol with that of 1,25D in animal models of disease and, in particular, determine whether triciferol, like other 1,25D analogs (43), lacks the undesirable calcemic properties of 1,25D.

In conclusion, the above studies demonstrate the synthetic feasibility of combining HDAC inhibition with VDR agonism in 1,25D analogs to enhance their therapeutic potential. Triciferol is unique in that it is a fully merged structure targeting two radically different and biochemically distinct proteins (a metalloenzyme and a nuclear receptor ligand binding domain), and provides proof-of-principle that a second biochemical activity can be incorporated into the agonist structure of a nuclear receptor ligand.

Materials and Methods

Synthesis of Triciferol. See *SI Materials and Methods* for a detailed protocol describing the synthesis of triciferol, including spectroscopic analysis of intermediates.

Molecular and Cell Biology. All cells used in this study were purchased from the American Type Culture Collection and cultured under recommended conditions. See *SI Materials and Methods, Cell and Molecular Biology* for details of all molecular and cell biology protocols, including tissue culture, cell viability assays, and microscopy, RT/PCR analysis, chromatin immunoprecipitation assays, Western blot analysis, and HDAC colorimetric assays.

ACKNOWLEDGMENTS. We thank Dr. Jing Liu and XiaoFeng Wang of the McGill University High Throughput Screening Facility for their assistance with the fluorescence polarization competition assay and Drs. Andreas Steinmeyer and Ekkehard May (Bayer Schering Pharma) for their generous gift of ZK159222. This work was supported by a scholarship from the Montreal Centre for Experimental Therapeutics in Cancer (L.E.T.-M.), a McGill University Health Centre scholarship (to B.D.), a Natural Sciences and Engineering Research Council Postgraduate Scholarship (to J.H.), a Natural Sciences and Engineering Research Council Undergraduate Summer Research Award (to X.L.), and a Proof-of-Principle grant from the Canadian Institutes of Health Research (to J.H.W. and J.L.G.). J.H.W. is a Chercheur-Boursier National of the Fonds de Recherche en Santé du Québec.

1. Feldman D, Glorieux FH, Pike JW (1997) *Vitamin D* (Academic, New York).
2. Lin R, White JH (2004) The pleiotropic actions of vitamin D. *BioEssays* 26:21–28.
3. Masuda S, Jones G (2006) Promise of vitamin D analogues in the treatment of hyperproliferative conditions. *Mol Cancer Ther* 5:797–808.
4. Lim WC, Hanauer SB, Li YC (2005) Mechanisms of disease: Vitamin D and inflammatory bowel disease. *Nature Clin Practice Gastroenterol Hepatol* 2:308–315.
5. Wang TT, *et al.* (2004) 1,25-dihydroxyvitamin D3 is a direct inducer of antimicrobial peptide gene expression. *J Immunol* 173:2909–2912.
6. Zasloff M (2005) Sunlight, vitamin D, and the innate immune defenses of the human skin. *J Invest Dermatol* 125:XVI–XVII.
7. Liu PT, Krutzik SR, Modlin RL (2007) Therapeutic implications of the TLR and VDR partnership. *Trends Mol Med* 13:117–124.
8. Liu PT, *et al.* (2006) Toll-like receptor triggering of a vitamin D-mediated human antimicrobial response. *Science* 311:1770–1773.
9. Khanim FL, *et al.* (2004) Altered SMRT levels disrupt vitamin D-3 receptor signalling in prostate cancer cells. *Oncogene* 23:6712–6725.
10. Kim SC, *et al.* (2006) Substrate and functional diversity of lysine acetylation revealed by a proteomics survey. *Mol Cell* 23:607–618.
11. McLaughlin F, La Thangue NB (2004) Histone deacetylase inhibitors open new doors in cancer therapy. *Biochem Pharm* 68:1139–1144.
12. Villar-Garea A, Esteller M (2004) Histone deacetylase inhibitors: Understanding a new wave of anticancer agents. *Int J Cancer* 112:171–178.
13. Xu WS, Parmigiani RB, Marks PA (2007) Histone deacetylase inhibitors: Molecular mechanisms of action. *Oncogene* 26:5541–5552.
14. Wang Z, Bennett EM, Wilson DJ, Salomon C, Vince R (2007) Rationally designed dual inhibitors of HIV reverse transcriptase and integrase. *J Med Chem* 50:3416–3419.
15. Tsalamandris C, Panagiotopoulos S, Sinha A, Cooper ME, Jerums G (1994) Complementary effects of pravastatin and nicotinic acid in the treatment of combined hyperlipidaemia in diabetic and non-diabetic patients. *J Cardiovasc Risk* 1:231–239.
16. Morphy R, Rankovic Z (2005) Designed multiple ligands. An emerging drug discovery paradigm. *J Med Chem* 48:6523–6543.
17. Meunier B (2008) Hybrid Molecules with a Dual Mode of Action: Dream or Reality. *Acc Chem Res* 41:69–77.
18. Bralet J, Schwartz J-C (2001) Vasopeptidase inhibitors: An emerging class of cardiovascular drugs. *Trends Pharm Sci* 22:16–109.

19. Rochel N, Wurtz JM, Mitschler A, Klaholz B, Moras D (2000) The crystal structure of the nuclear receptor for vitamin D bound to its natural ligand. *Mol Cell* 5:173–179.
20. Hansen CM, Hamberg KJ, Binderup E, Binderup L (2000) Seocalcitol (EB1089): A vitamin D analogue of anti-cancer potential. Background, design, synthesis, pre-clinical and clinical evaluation. *Curr Pharm Des* 6:803–828.
21. Tocchini-Valentini G, Rochel N, Wurtz JM, Moras D (2004) Crystal structures of the vitamin D nuclear receptor liganded with the vitamin D side chain analogues calcipotriol and seocalcitol, receptor agonists of clinical importance. Insights into a structural basis for the switching of calcipotriol to a receptor antagonist by further side chain modification. *J Med Chem* 47:1956–1961.
22. Monneret C (2005) Histone deacetylase inhibitors. *Eur J Med Chem* 40:1–13.
23. Marson CM, *et al.* (2004) Stereodefined and polyunsaturated inhibitors of histone deacetylase based on (2E,4E)-5-arylpenta-2,4-dienoic acid hydroxyamides. *Biorg Med Chem Lett* 14:2477–2481.
24. Suzuki T, Miyata N (2005) Non-hydroxamate histone deacetylase inhibitors. *Curr Med Chem* 12:2867–2880.
25. Morris GM, *et al.* (1998) Automated docking using a Lamarckian genetic algorithm and an empirical binding free energy function. *J Comp Chem* 19:1639–1662.
26. Corbeil CR, Englebienne P, Moitessier N (2007) Docking ligands into flexible and solvated macromolecules. 1. Development and validation of FITTED 1.0. *J Chem Info Mod* 47:435–449.
27. Fujishima T, *et al.* (2000) Efficient synthesis and biological evaluation of all A-ring diastereomers of 1α,25-dihydroxyvitamin D3 and its 20-epimer. *Biorg Med Chem Lett* 8:123–134.
28. Perlman KL, Sicinski RR, Schnoes HK, DeLuca HF (1990) 1α,25-Dihydroxy-19-norvitamin D3, a novel vitamin D-related compound with potential therapeutic activity. *Tetrahedron Lett* 31:1823–1824.
29. St John LS, Sauter ER, Herlyn M, Litwin S, Adler-Storthz K (2000) Endogenous p53 gene status predicts the response of human squamous cell carcinomas to wild-type p53. *Cancer Gene Ther* 7:749–756.
30. Akutsu N, *et al.* (2001) Regulation of gene expression by 1α,25-dihydroxyvitamin D_3 and its analog EB1089 under growth inhibitory conditions in squamous carcinoma cells. *Mol Endocrinol* 15:1127–1139.
31. Lin R, *et al.* (2002) Expression profiling in squamous carcinoma cells reveals pleiotropic effects of vitamin D3 signaling on cell proliferation, differentiation and immune system regulation. *Mol Endocrinol* 16:1243–1256.
32. Wang TT, *et al.* (2005) Large-scale *in silico* and microarray-based genomic screening of 1,25-dihydroxyvitamin D_3 target genes. *Mol Endocrinol* 19:2685–2695.
33. Fan GK, Chen J, Ping F, Geng Y (2006) Immunohistochemical analysis of P57(kip2), p53 and hsp60 expressions in premalignant and malignant oral tissues. *Oral Oncology* 42:147–153.
34. Chen KS, DeLuca HF (1995) Cloning of the human 1 alpha,25-dihydroxyvitamin D-3 24-hydroxylase gene promoter and identification of two vitamin D-responsive elements. *Biochim Biophys Acta* 1263:1–9.
35. Anzick SL, *et al.* (1997) AIB1, a steroid receptor coactivator amplified in breast and ovarian cancer *Science* 277:965–968.
36. Wegener D, Wirsching F, Riester D, Schwienhorst A (2003) A fluorogenic histone deacetylase assay well suited for high-throughput activity screening. *Chem and Biol* 10:61–68.
37. Bursch W, *et al.* (1996) Active cell death induced by the anti-estrogens tamoxifen and ICI 164 384 in human mammary carcinoma cells (MCF-7) in culture: The role of autophagy. *Carcinogenesis* 17:1595–1607.
38. Hoyer-Hansen M, Bastholm L, Mathiasen IS, Elling F, Jaattela M (2005) Vitamin D analog EB1089 triggers dramatic lysosomal changes and Beclin 1-mediated autophagic cell death. *Cell Death Diff*, 12:1297–1309.
39. Minucci S, Pelicci PG (2006) Histone deacetylase inhibitors and the promise of epigenetic (and more) treatments for cancer. *Nat Rev Cancer* 6:38–51.
40. Drummond DC, *et al.* (2004) Clinical development of histone deacetylase inhibitors as anticancer agents. *Ann Rev Pharmacol Toxicol* 45:495–528.
41. Alao JP, *et al.* (2004) Histone deacetylase inhibitor trichostatin A represses estrogen receptor alpha-dependent transcription and promotes proteasomal degradation of cyclin D1 in human breast carcinoma cell lines. *Clin Cancer Res* 10:8094–8104.
42. Jang ER, *et al.* (2004) The histone deacetylase inhibitor trichostatin A sensitizes estrogen receptor alpha-negative breast cancer cells to tamoxifen. *Oncogene* 23:1724–1736.
43. Ma YF, *et al.* (2006) Identification and characterization of noncalcemic, tissue-selective, nonsecosteroidal vitamin D receptor modulators. *J Clin Invest* 116:892–904.